Release Note of Bias-corrected FTS SWIR Level 2 CO_2 Product (V02.97/V02.98) for General Users

August 26, 2021
Revised on August 8, 2023
NIES GOSAT Project

1. Introduction

The NIES GOSAT Project has produced the FTS SWIR Level 2 CO_2 products (hereinafter referred to as "SWIR L2 CO_2 product") from the FTS Level 1B products (hereinafter referred to as "FTS L1B data") provided by JAXA. The SWIR L2 CO_2 product (V02.90/V02.91) with the FTS L1B data (V220.220/V220.221) as the input for the entire observation period since April 23, 2009 has been released to General Users (GU). Using the ground-based observation data of the Total Carbon Column Observing Network (TCCON), bias-corrections are conducted on the column-averaged concentration of carbon dioxide (XCO_2) of the SWIR L2 CO_2 product (V02.90/V02.91), and the results have been being released as the bias-corrected FTS SWIR Level 2 CO_2 products (hereinafter referred to as "corrected SWIR L2 CO_2 product") (V02.95/V02.96) to GU.
Regardless of before and after bias-corrections, the problem was found that the annual growth rate of XCO_2 over ocean is lower than that of TCCON data or ground station data. In order to solve this problem, additional bias-corrections are conducted on only the bias-corrected XCO_2 over ocean, and the results are upgraded as the corrected SWIR L2 CO_2 product (V02.97/V02.98) and released to GU. The bias-corrections results of XCO_2 over land of this version (V02.97/V02.98) are the same as those of the previous version (V02.95/V02.96). The entire observation period since April 23, 2009 will be covered. Accordingly, the production of the corrected SWIR L2 CO_2 product (V02.96) had finished on July 31, 2021.

2. Match-up Between SWIR L2 CO_2 Product and TCCON Data

We selected the TCCON data corresponding to the observation time and the observation position of each FTS scan stored in the SWIR L2 CO_2 product from 2009 to 2018 under the following criteria (This selection is called “match-up”):

(1) Select the FTS scan with the center position of the FTS IFOV within 2 degrees (land with Gain H) or 5 degrees (land with Gain M and ocean with Gain H/M) from the latitude and longitude of the TCCON site depending on the observation area (land and ocean) and the observation gain (H and M) of the FTS, and with the difference between the average altitude of the FTS IFOV and the altitude of the TCCON site within 2 km;

(2) Select the data of the TCCON site located at the shortest distance from the center position of the FTS IFOV;

(3) Calculate the mean value of the TCCON data within 30 minutes before and after the observation time of the FTS scan.

The TCCON data can be obtained from the TCCON Data Archive website. However, they are updated irregularly and may be different depending on the acquisition time.

Table 2-1 is the list of the TCCON data referenced in the bias-correction processing. The FTS scan numbers of match-up results for land and ocean with each observation gain are shown in Table 2-2, where the land fraction within FTS IFOV of 100% is defined as “land” and 0% as “ocean”; the mixed of 60% or more and less than 100% are excluded.

Table 2-1: TCCON data referenced in bias-correction processing

Site code	Site name	Lat. (deg. N)	Lon. (deg. E)	Alt. (km)	File name
ae	Ascension Island	−7.92	−14.33	0.03	ae20120522_20181031.public.nc
an	Anmyeondo	36.54	126.33	0.03	an20150202_20180418.public.nc
bi	Białystok	53.23	23.02	0.13	bi20090301_20181001.public.nc
br	Bremen	53.10	8.85	0.03	br20100122_20190425.public.nc
bu	Burgos	18.53	120.65	0.04	bu20170303_20190426.public.nc
ci	Pasadena	34.14	−118.13	0.24	ci20120920_20200101.public.nc
db	Darwin	−12.43 −12.46	130.89 130.93	0.03 0.04	db20050828_20190328.public.nc
df	Edwards	34.96	−117.88	0.70	df20130720_20200101.public.nc
et	East Trout Lake	54.36 54.35	−104.99 −104.99	0.50 0.50	et20161007_20191229.public.nc
eu	Eureka	80.05	−86.42	0.61	eu20100724_20190815.public.nc
fc	Four Corners	36.80	−108.48	1.64	fc20130316_20131004.public.nc
gm	Garmisch	47.48	11.06	0.75	gm20070716_20191018.public.nc
hf	Hefei	31.90	117.17	0.04	hf20150918_20161231.public.nc
if	Indianapolis	39.86	−86.00	0.27	if20120823_20121201.public.nc
iz	Izaña	28.30 28.31	−16.48 −16.50	2.37 2.37	iz20070518_20200128.public.nc
jc	JPL	34.20	−118.18	0.39	jc20070731_20080622.public.nc
jf	JPL	34.20	−118.18	0.39	jf20110519_20180514.public.nc
js	Saga	33.24	130.29	0.01	js20110728_20191102.public.nc
ka	Karlsruhe	49.10	8.44	0.11	ka20100419_20200124.public.nc
lh	Lauder	−45.05 −45.04	169.68 169.68	0.37 0.37	lh20040629_20101209.public.nc
ll	Lauder	−45.04	169.68	0.37	ll20100202_20181031.public.nc
lr	Lauder	−45.04	169.68	0.37	lr20181003_20191102.public.nc
ma	Manaus	−3.21	−60.60	0.05	ma20141001_20150624.public.nc
oc	Lamont	36.60	−97.49	0.32	oc20080706_20200101.public.nc
or	Orléans	47.97	2.11	0.13	or20090829_20190430.public.nc
pa	Park Falls	45.94	−90.27	0.44	pa20040602_20191222.public.nc
pr	Paris	48.85	2.36	0.06	pr20140923_20190426.public.nc
ra	Réunion Island	−20.90	55.49	0.09	ra20110916_20200131.public.nc
rj	Rikubetsu	43.46	143.77	0.38	rj20131116_20190424.public.nc
so	Sodankylä	67.37	26.63	0.19	so20090516_20191030.public.nc
sp	Ny-Ålesund	78.92	11.92	0.02	sp20140406_20190429.public.nc
tk	Tsukuba	36.05	140.12	0.03	tk20110804_20190423.public.nc
wg	Wollongong	−34.41	150.88	0.03	wg20080626_20190430.public.nc
zs	Zugspitze	47.42	10.98	2.96	zs20150424_20191017.public.nc

Table 2-2: Match-up FTS scan numbers of SWIR L2 CO_2 product [2009-2018]

Site code	Site name	Land		Ocean	
		Gain H	Gain M	Gain H	Gain M
ae	Ascension Island	0	0	1,090	0
an	Anmyeondo	12	0	6	0
bi	Białystok	140	0	0	0
br	Bremen	27	0	1	0
bu	Burgos	8	0	36	0
ci	Pasadena	1,589	498	13	0
db	Darwin	335	0	259	0
df	Edwards	183	1,442	0	0
et	East Trout Lake	4	0	0	0
eu	Eureka	5	0	0	0
fc	Four Corners	23	1	0	0
gm	Garmisch	265	0	20	0
hf	Hefei	8	0	9	0
if	Indianapolis	40	0	0	0
iz	Izaña	0	0	0	0
jc	JPL	0	0	0	0
jf	JPL	616	622	9	0
js	Saga	224	0	67	0
ka	Karlsruhe	212	0	0	0
lh	Lauder	10	0	1	0
ll	Lauder	329	0	35	0
lr	Lauder	12	0	11	0
ma	Manaus	0	0	0	0
oc	Lamont	1,233	0	0	0
or	Orléans	341	0	0	0
pa	Park Falls	139	0	2	0
pr	Paris	73	0	0	0
ra	Réunion Island	2	0	649	0
rj	Rikubetsu	88	0	69	0
so	Sodankylä	136	0	0	0
sp	Ny-Ålesund	0	0	0	0
tk	Tsukuba	1,030	0	13	0
wg	Wollongong	489	0	358	0
zs	Zugspitze	19	0	0	0
Total		7,592	2,563	2,648	0

3. Method of Bias-correction

3.1 Regression Analysis

Based on the match-up results between the SWIR L2 CO_2 product and the TCCON data from 2009 to 2018, the multiple regression analyses were performed on XCO_2 by categories of land (Gain H and Gain M) and ocean (Gain H), using the following regression equation, which includes explanatory variables described in Inoue et al. (2016).

$$\begin{aligned}\mathrm{XCO}_2^{\mathrm{Bias-corrected}} = {} & \mathrm{XCO}_2 + C_1(\mathrm{AOT} - \overline{\mathrm{AOT}}) + C_2(\Delta P_S - \overline{\Delta P_S}) \\ & + C_3(\mathrm{Airmass} - \overline{\mathrm{Airmass}}) + C_4(\mathrm{Albedo\_O_2} - \overline{\mathrm{Albedo\_O_2}}) + C_5\end{aligned}$$

The parameters used for the explanatory variables in this regression equation are shown in Table 3.1-1. For each explanatory variable, the deviation from the mean value of all match-up FTS scans was used.

For land (Gain H), the multiple regression analyses were performed considering the weight corresponding to the match-up FTS scan number of each TCCON site. For land (Gain M) and ocean (Gain H), however, the weight was not considered.

The errors (variance σ^2) of the bias-corrected XCO_2 were calculated by the following equation.

$$\begin{aligned}(\sigma \mathrm{XCO}_2^{\mathrm{Bias-corrected}})^2 = {} & (\sigma \mathrm{XCO}_2^{\mathrm{smoothing\_error}})^2 + (\sigma \mathrm{XCO}_2^{\mathrm{retrieval\_noise}})^2 \\ & + (\sigma \mathrm{XCO}_2^{\mathrm{interference\_error}})^2 + {\sigma_1}^2(\mathrm{AOT} - \overline{\mathrm{AOT}})^2 \\ & + {\sigma_2}^2(\Delta P_S - \overline{\Delta P_S})^2 + {\sigma_3}^2(\mathrm{Airmass} - \overline{\mathrm{Airmass}})^2 \\ & + {\sigma_4}^2(\mathrm{Albedo\_O_2} - \overline{\mathrm{Albedo\_O_2}})^2 + {\sigma_5}^2\end{aligned}$$

The above multiple regression analyses are the same as those of the previous version (V02.95/V02.96). In this version (V02.97/V02.98), the additional simple regression analysis was performed on bias-corrected XCO_2 using the following regression equation only for ocean (Gain H).

$$\mathrm{XCO}_2^{\mathrm{Bias-corrected\_2}} = \mathrm{XCO}_2^{\mathrm{Bias-corrected}} + C_1'(\mathrm{XCO}_2^{\mathrm{Bias-corrected}} - \overline{\mathrm{XCO}_2^{\mathrm{Bias-corrected}}}) + C_2'$$

The parameter used for the explanatory variable in this regression equation is shown in Table 3.1-2. The weight corresponding to the match-up FTS scan number of each TCCON site was not considered.

The errors (variance σ^2) of the bias-corrected XCO_2 (added) over ocean (Gain H) were calculated by the following equation.

$$\begin{aligned}(\sigma \mathrm{XCO}_2^{\mathrm{Bias-corrected\_2}})^2 = {} & (1 + C_1')^2(\sigma \mathrm{XCO}_2^{\mathrm{Bias-corrected}})^2 \\ & + (\sigma_1')^2(\mathrm{XCO}_2^{\mathrm{Bias-corrected}} - \overline{\mathrm{XCO}_2^{\mathrm{Bias-corrected}}})^2 + (\sigma_2')^2\end{aligned}$$

Table 3.1-1: Parameters used for explanatory variables in regression equation (XCO_2)

Parameter	Description	Land		Ocean
		Gain H	Gain M	Gain H
AOT	Aerosol optical thickness retrieved simultaneously by FTS SWIR L2 processing	–	–	✓
ΔP_S	Difference between surface pressure retrieved simultaneously by FTS SWIR L2 processing and *a priori* surface pressure	✓	✓	✓
Airmass	Airmass calculated by 1/cos (Solar zenith angle) + 1/cos (Satellite zenith angle)	✓	✓	–
Albedo_O_2	Surface albedo of O_2A-band retrieved simultaneously by FTS SWIR L2 processing	✓	–	–

Table 3.1-2: Parameter used for explanatory variable in regression equation (Bias-corrected XCO_2)

Parameter	Description	Land		Ocean
		Gain H	Gain M	Gain H
$XCO_2^{Bias-corrected}$	Bias-corrected XCO_2	–	–	✓

3.2 Bias-correction Processing

We conducted comprehensive bias-correction processing using these regression analyses results. The differences in XCO_2 between the SWIR L2 CO_2 product and the TCCON data, the partial regression coefficients and the intercepts obtained by these regression analyses, and the differences in XCO_2 between the corrected SWIR L2 CO_2 product and the TCCON data are summarized in Table 3.2-1. Note that the empirical bias-correction processing using the regression analyses results of the land (Gain H and Gain M) are also applied to the FTS scans of the mixed (land fraction within FTS IFOV of 60% or more and less than 100%), respectively. The empirical bias-correction processing using the regression analyses results of the ocean (Gain H) is applied to the FTS scans of the ocean (Gain M). Furthermore, we apply the bias-correction processing determined from the match-up results from 2009 to 2018 to the FTS scans of the SWIR L2 CO_2 product after 2019, and produce the corrected SWIR L2 CO_2 product.

For 2019, the match-up FTS scan numbers of SWIR L2 CO_2 product are shown in Table 3.2-2, and these bias-correction processing results are summarized in Table 3.2-3.

The scatter plots of XCO_2 over land (Gain H and Gain M) and ocean (Gain H) between the SWIR L2 CO_2 product and the TCCON data, the corrected SWIR L2 CO_2 product and the TCCON data from 2009 to 2018 and 2019 are shown separately for land (Gain H and Gain M) and ocean (Gain H) in Figures 3.2-1 to 3.2-6.

Table 3.2-1: Regression analyses and bias-correction processing results of SWIR L2 CO_2 product (XCO_2) [2009-2018]

			Land		Ocean
			Gain H	Gain M	Gain H
SWIR L2 CO_2 product	Mean difference from TCCON data* (ppm)		−0.302	1.452	−1.285
	SD of difference from TCCON data* (ppm)		2.200	2.209	1.861
	Correlation coefficient with TCCON data		0.949	0.904	0.935
Multiple regression analysis	PRC	C_1 (ppm)	−	−	−16.425
		C_2 (ppm/hPa)	0.235	0.263	0.245
		C_3 (ppm)	−0.119	−1.265	−
		C_4 (ppm)	3.466	−	−
	Intercept	C_5 (ppm)	0.280	−1.452	1.285
	SD of PRC	σ_1 (ppm)	−	−	1.415
		σ_2 (ppm/hPa)	0.006	0.015	0.008
		σ_3 (ppm)	0.066	0.105	−
		σ_4 (ppm)	0.519	−	−
	SD of intercept	σ_5 (ppm)	0.023	0.040	0.031
	Adjusted R-square		0.163	0.162	0.281
Simple regression analysis	PRC	C'_1 (ppm/ppm)	−	−	0.073
	Intercept	C'_2 (ppm)	−	−	−0.000
	SD of PRC	σ'_1 (ppm/ppm)	−	−	0.004
	SD of intercept	σ'_2 (ppm)	−	−	0.019
Corrected SWIR L2 CO_2 product	Mean difference from TCCON data† (ppm)		−0.022	0.000	0.000
	SD of difference from TCCON data† (ppm)		2.015	2.022	1.644
	Correlation coefficient with TCCON data		0.956	0.920	0.952

* Value of SWIR L2 CO_2 product minus TCCON data

† Value of corrected SWIR L2 CO_2 product minus TCCON data

Table 3.2-2: Match-up FTS scan numbers of SWIR L2 CO_2 product [2019]

Site code	Site name	Land		Ocean	
		Gain H	Gain M	Gain H	Gain M
ae	Ascension Island	0	0	0	0
an	Anmyeondo	0	0	0	0
bi	Białystok	0	0	0	0
br	Bremen	1	0	0	0
bu	Burgos	12	0	20	0
ci	Pasadena	372	26	2	0
db	Darwin	0	0	1	0
df	Edwards	115	643	0	0
et	East Trout Lake	0	0	0	0
eu	Eureka	3	0	0	0
fc	Four Corners	0	0	0	0
gm	Garmisch	36	0	2	0
hf	Hefei	0	0	0	0
if	Indianapolis	0	0	0	0
iz	Izaña	0	0	0	0
jc	JPL	0	0	0	0
jf	JPL	0	0	0	0
js	Saga	35	0	3	0
ka	Karlsruhe	42	0	0	0
lh	Lauder	0	0	0	0
ll	Lauder	0	0	0	0
lr	Lauder	79	0	4	0
ma	Manaus	0	0	0	0
oc	Lamont	100	0	0	0
or	Orléans	41	0	0	0
pa	Park Falls	23	0	0	0
pr	Paris	14	0	0	0
ra	Reéunion Island	0	0	110	0
rj	Rikubetsu	1	0	0	0
so	Sodankylä	5	0	0	0
sp	Ny-Ålesund	0	0	0	0
tk	Tsukuba	113	0	0	0
wg	Wollongong	8	0	18	0
zs	Zugspitze	6	0	0	0
Total		1,006	669	160	0

Table 3.2-3: Bias-correction processing results of SWIR L2 CO_2 product (XCO_2) [2019]

		Land		Ocean
		Gain H	Gain M	Gain H
SWIR L2 CO_2 product	Mean difference from TCCON data* (ppm)	−0.812	1.745	−2.079
	SD of difference from TCCON data* (ppm)	2.185	2.010	2.158
	Correlation coefficient with TCCON data	0.693	0.517	0.665
Corrected SWIR L2 CO_2 product	Mean difference from TCCON data† (ppm)	−0.413	0.287	−0.206
	SD of difference from TCCON data† (ppm)	2.018	1.688	1.731
	Correlation coefficient with TCCON data	0.714	0.636	0.717

* Value of SWIR L2 CO_2 product minus TCCON data

† Value of corrected SWIR L2 CO_2 product minus TCCON data

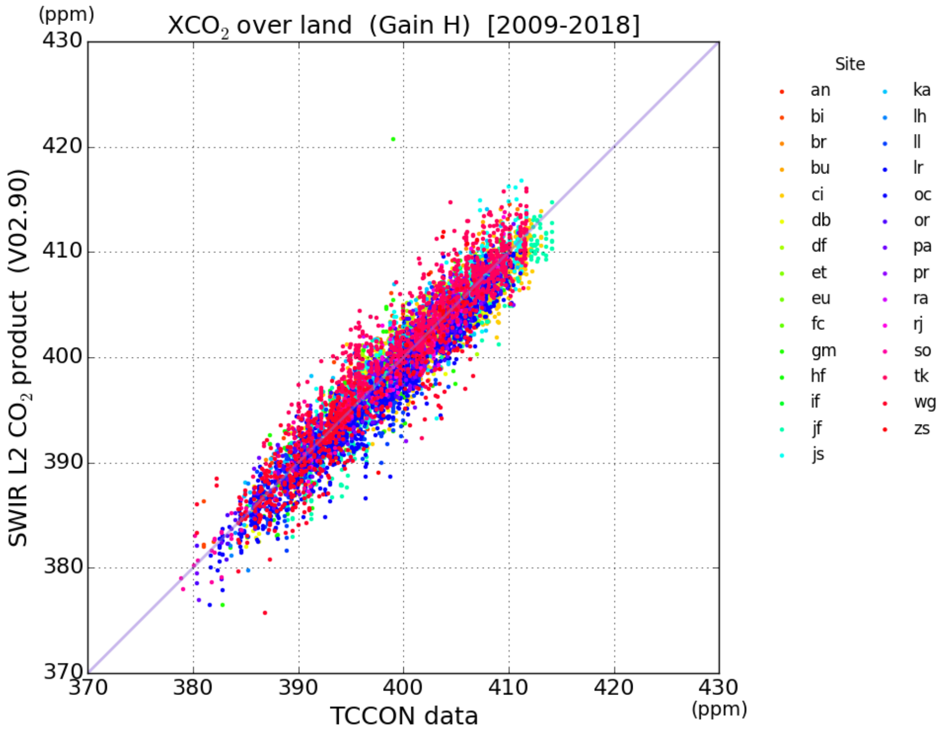

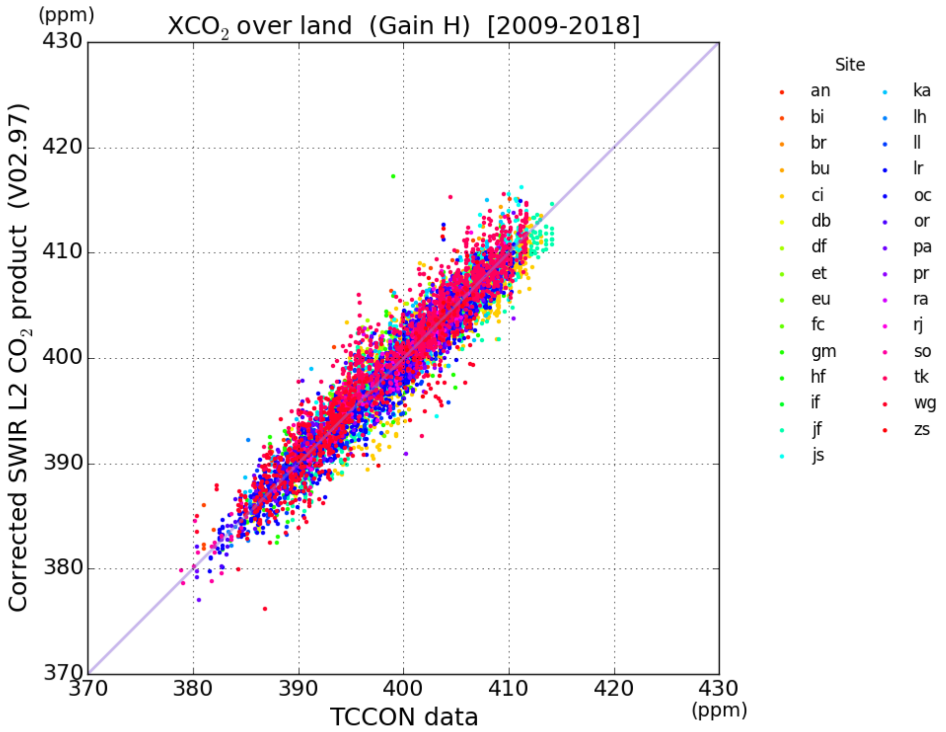

Figure 3.2-1: Scatter plots of XCO_2 over land (Gain H) with TCCON data [2009-2018]
(Top: SWIR L2 CO_2 product V02.90, Bottom: Corrected SWIR L2 CO_2 product V02.97)

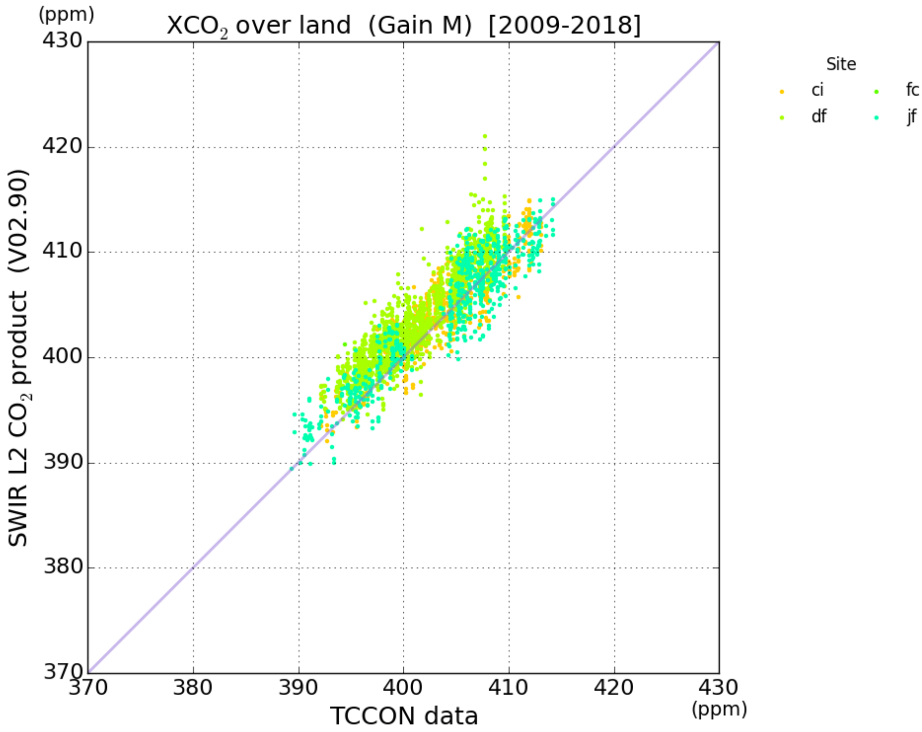

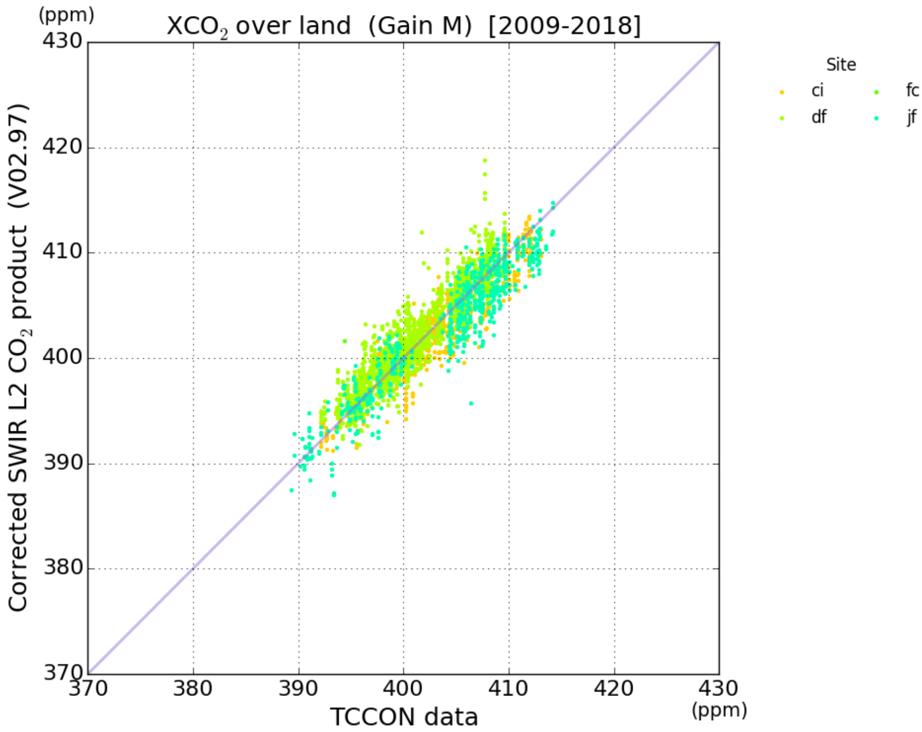

Figure 3.2-2: Scatter plots of XCO_2 over land (Gain M) with TCCON data [2009-2018]
(Top: SWIR L2 CO_2 product V02.90, Bottom: Corrected SWIR L2 CO_2 product V02.97)

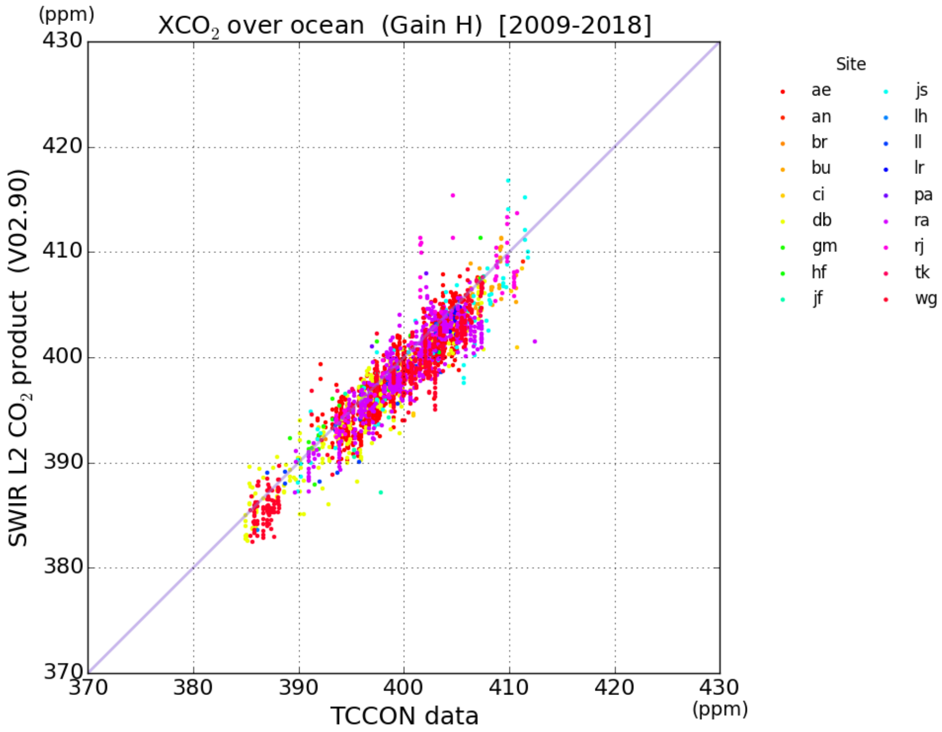

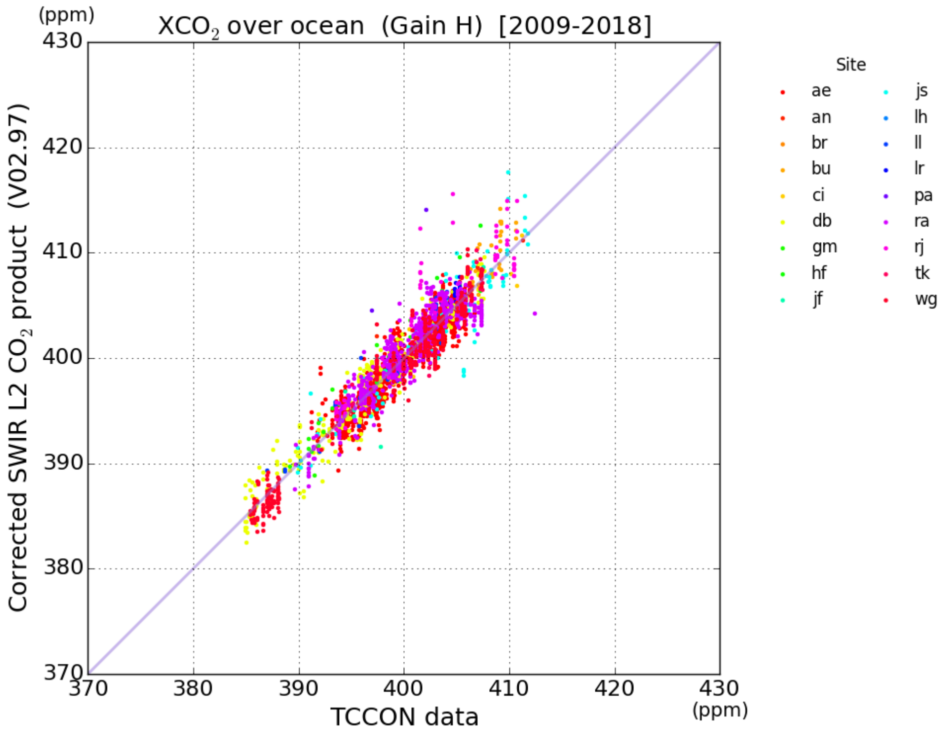

Figure 3.2-3: Scatter plots of XCO_2 over ocean (Gain H) with TCCON data [2009-2018]
(Top: SWIR L2 CO_2 product V02.90, Bottom: Corrected SWIR L2 CO_2 product V02.97)

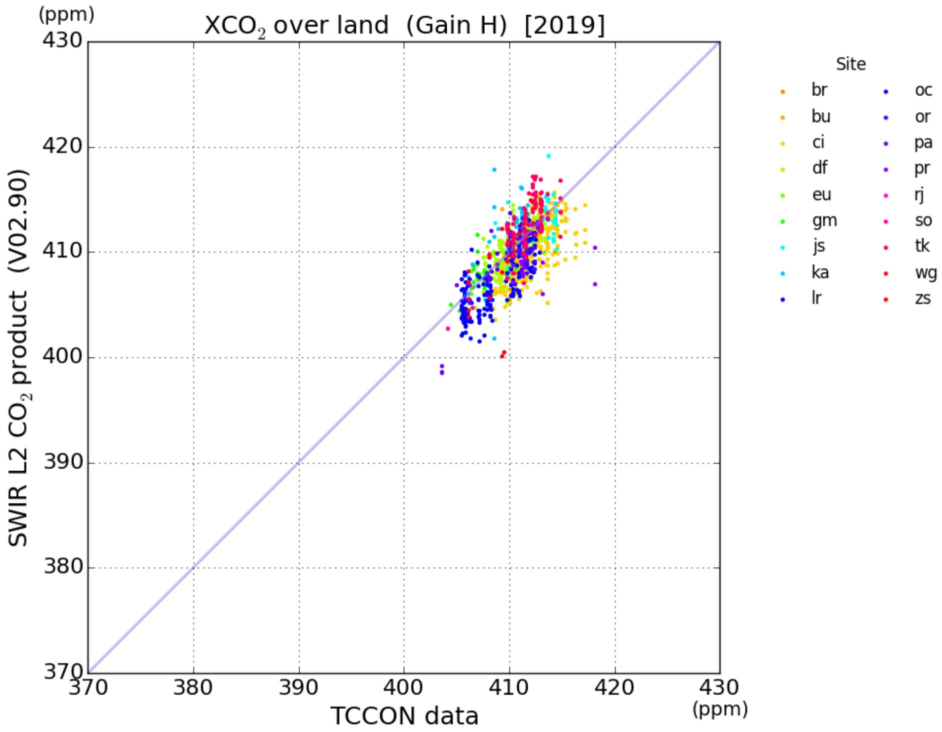

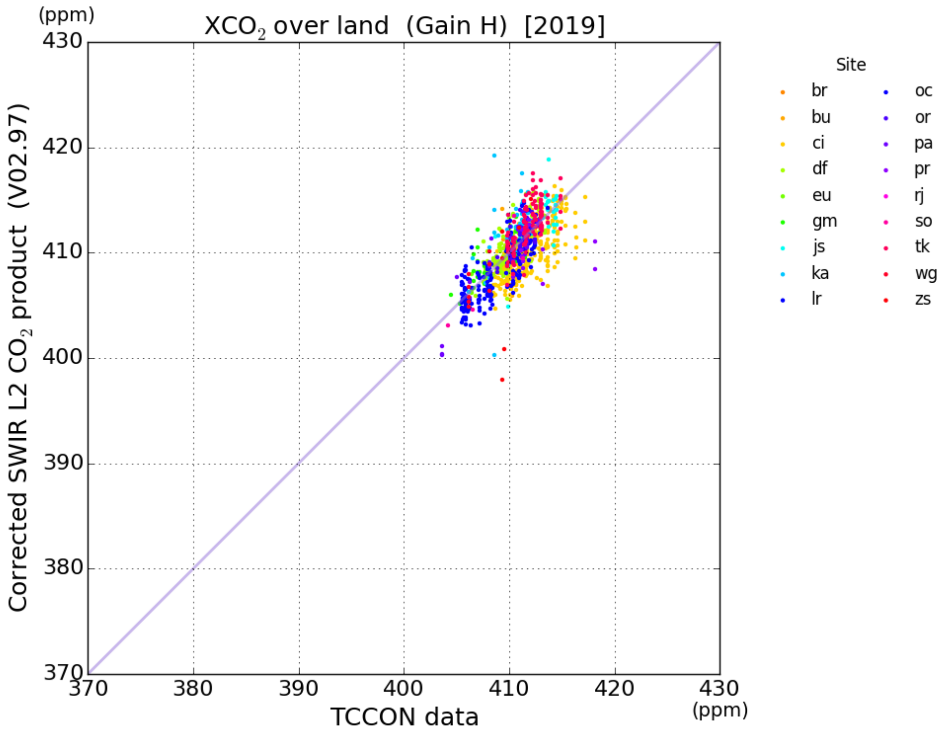

Figure 3.2-4: Scatter plots of XCO_2 over land (Gain H) with TCCON data [2019]
(Top: SWIR L2 CO_2 product V02.90, Bottom: Corrected SWIR L2 CO_2 product V02.97)

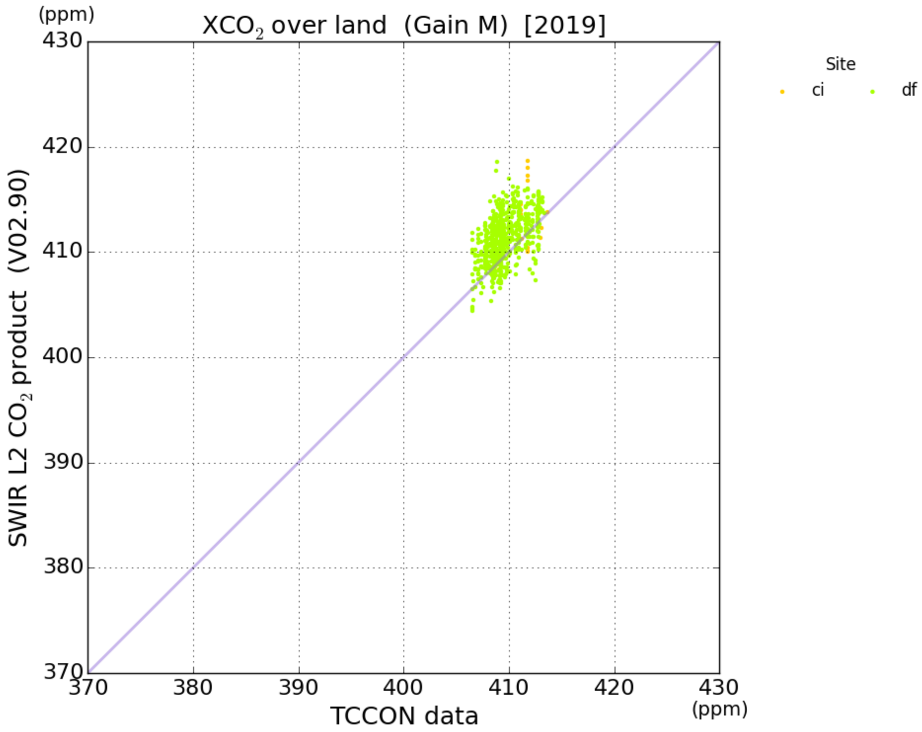

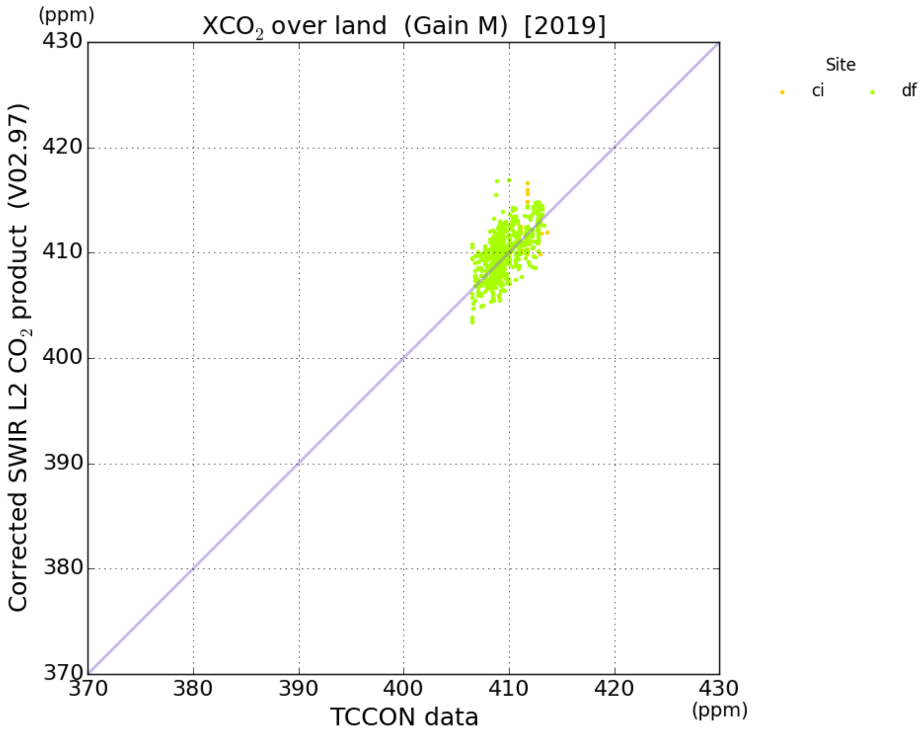

Figure 3.2-5: Scatter plots of XCO_2 over land (Gain M) with TCCON data [2019]
(Top: SWIR L2 CO_2 product V02.90, Bottom: Corrected SWIR L2 CO_2 product V02.97)

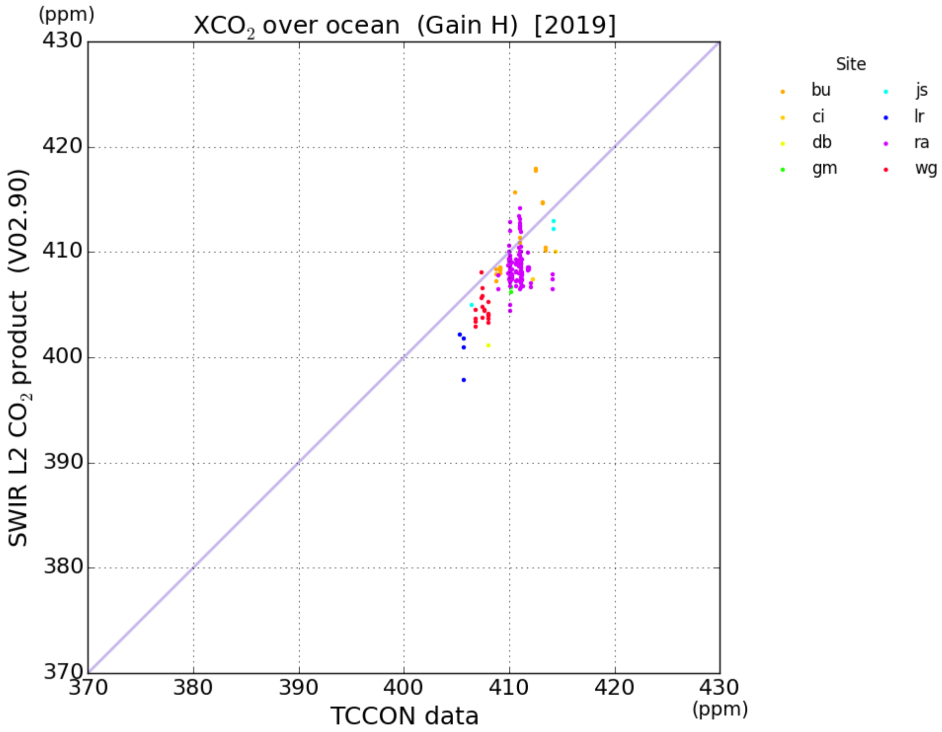

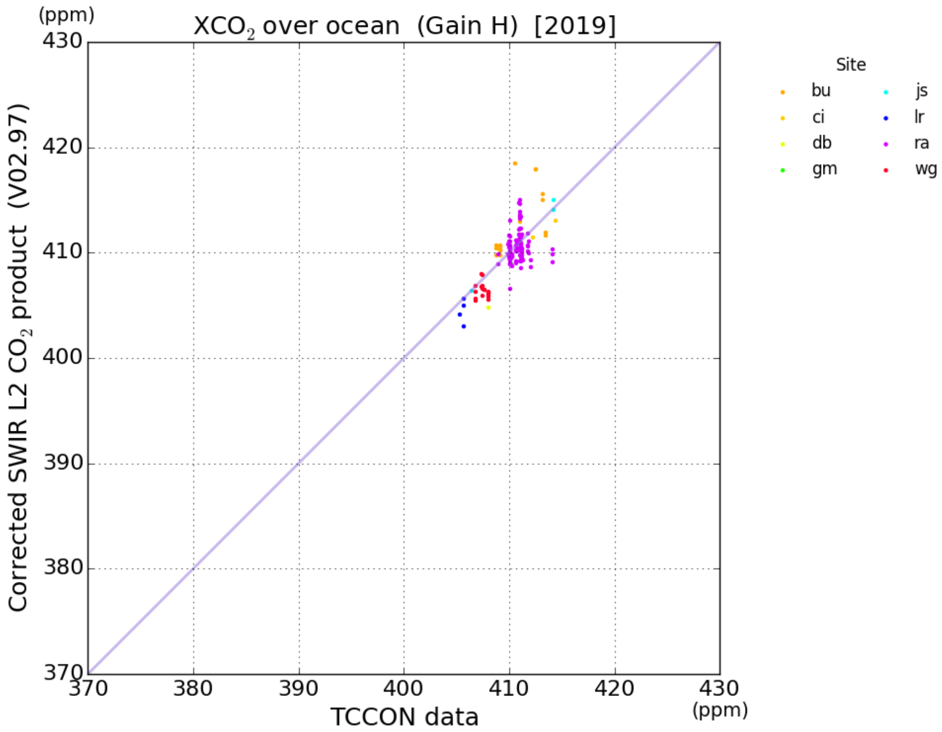

Figure 3.2-6: Scatter plots of XCO_2 over ocean (Gain H) with TCCON data [2019]
(Top: SWIR L2 CO_2 product V02.90, Bottom: Corrected SWIR L2 CO_2 product V02.97)

4. Annual Growth Rate

We performed time series regression analyses on XCO_2 of the SWIR CO_2 product (V02.90) and the corrected SWIR CO_2 products (V02.95, V02.97) from 2009 to 2018, and the SWIR CO_2 product (V02.90/V02.91) and the corrected SWIR CO_2 products (V02.95/V02.96, V02.97/V02.98) from 2009 to 2020 by separately for land (Gain H and Gain M) and ocean (Gain H). The calculated mean annual growth rates of XCO_2 are summarized in Tables 4-1 and 4-2. The results of these time series regression analyses are also shown in Figures 4-1 and 4-2.

Table 4-1: Mean annual growth rate of XCO_2 [2009-2018]

<table>
<tr><td colspan="2" rowspan="2"></td><td colspan="2">Land</td><td>Ocean</td></tr>
<tr><td>Gain H</td><td>Gain M</td><td>Gain H</td></tr>
<tr><td rowspan="3">Mean annual growth rate of XCO_2 (ppm/yr) [2009-2018]</td><td>SWIR L2 CO_2 product (V02.90)</td><td>2.31</td><td>2.38</td><td>2.23</td></tr>
<tr><td>Corrected SWIR L2 CO_2 product (V02.95)</td><td rowspan="2">2.33</td><td rowspan="2">2.37</td><td>2.24</td></tr>
<tr><td>Corrected SWIR L2 CO_2 product (V02.97)</td><td>2.40</td></tr>
</table>

Table 4-2: Mean annual growth rate of XCO_2 [2009-2020]

<table>
<tr><td colspan="2" rowspan="2"></td><td colspan="2">Land</td><td>Ocean</td></tr>
<tr><td>Gain H</td><td>Gain M</td><td>Gain H</td></tr>
<tr><td rowspan="3">Mean annual growth rate of XCO_2 (ppm/yr) [2009-2020]</td><td>SWIR L2 CO_2 product (V02.90/V02.91)</td><td>2.34</td><td>2.38</td><td>2.27</td></tr>
<tr><td>Corrected SWIR L2 CO_2 product (V02.95/V02.96)</td><td rowspan="2">2.36</td><td rowspan="2">2.38</td><td>2.27</td></tr>
<tr><td>Corrected SWIR L2 CO_2 product (V02.97/V02.98)</td><td>2.44</td></tr>
</table>

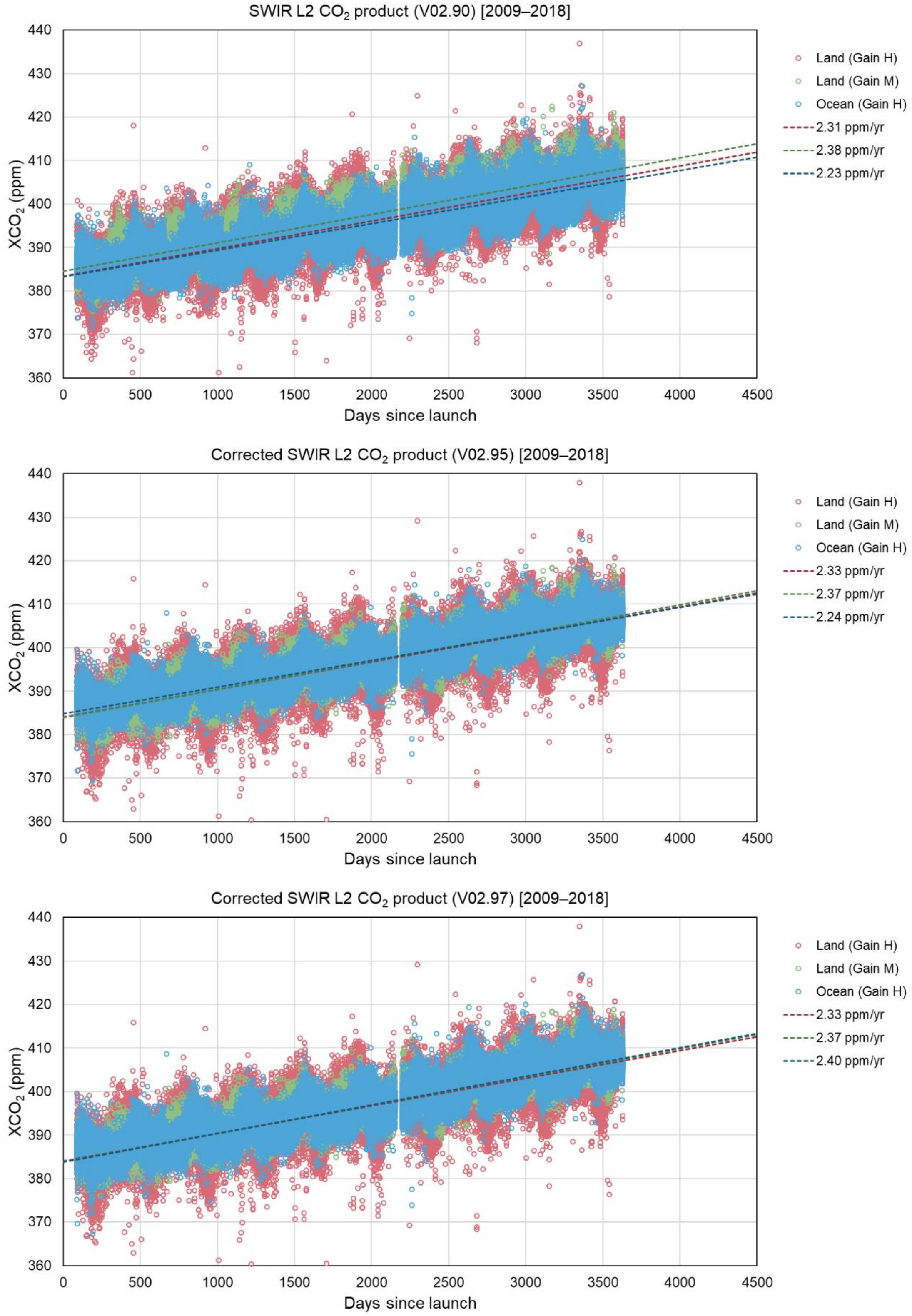

Figure 4-1: Time series regression analyses on XCO_2 [2009-2018]
(Top: SWIR L2 CO_2 product V02.90, Middle: Corrected SWIR L2 CO_2 product V02.95, Bottom: Corrected SWIR L2 CO_2 product V02.97)

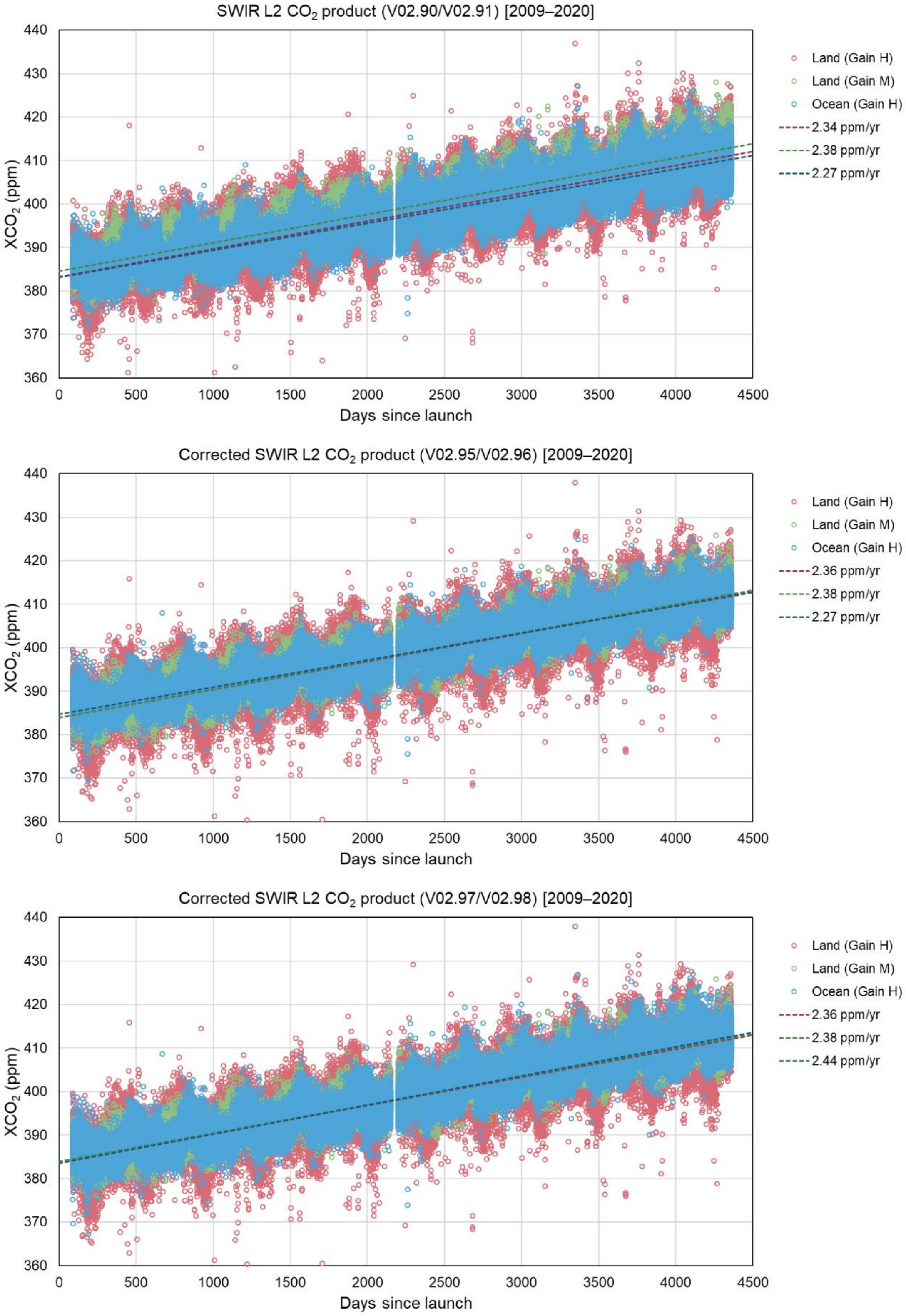

Figure 4-2: Time series regression analyses on XCO_2 [2009-2020]
(Top: SWIR L2 CO_2 product V02.90/V02.91, Middle: Corrected SWIR L2 CO_2 product V02.95/V02.96, Bottom: Corrected SWIR L2 CO_2 product V02.97/V02.98)

Reference

Inoue, M., Morino, I., Uchino, O., Nakatsuru, T., Yoshida, Y., Yokota, T., Wunch, D., Wennberg, P. O., Roehl, C. M., Griffith, D. W. T., Velazco, V. A., Deutscher, N. M., Warneke, T., Notholt, J., Robinson, J., Sherlock, V., Hase, F., Blumenstock, T., Rettinger, M., Sussmann, R., Kyrö, E., Kivi, R., Shiomi, K., Kawakami, S., De Mazière, M., Arnold, S. G., Feist, D. G., Barrow, E. A., Barney, J., Dubey, M., Schneider, M., Iraci, L. T., Podolske, J. R., Hillyard, P. W., Machida, T., Sawa, Y., Tsuboi, K., Matsueda, H., Sweeney, C., Tans, P. P., Andrews, A. E., Biraud, S. C., Fukuyama, Y., Pittman, J. V., Kort, E. A., and Tanaka, T.: Bias corrections of GOSAT SWIR XCO_2 and XCH_4 with TCCON data and their evaluation using aircraft measurement data, Atmos. Meas. Tech., 9, 3491-3512, https://doi.org/10.5194/amt-9-3491-2016, 2016.

Acronyms

AOT	Aerosol Optical Thickness
FTS	Fourier Transform Spectrometer
GOSAT	Greenhouse gases Observing SATellite
IFOV	Instantaneous Field Of View
JAXA	Japan Aerospace Exploration Agency
NIES	National Institute for Environmental Studies
PRC	Partial Regression Coefficient
SD	Standard Deviation
SWIR	Short-Wavelength InfraRed